Kidney International, Vol. 44 (1993), pp. 322–330

Calbindin-D_{28k} gene expression in the developing mouse kidney

LANTING LIU, S. TERENCE DUNN, SYLVIA CHRISTAKOS, OLIVIA HANSON-PAINTON, and JAMES E. BOURDEAU

Departments of Medicine, Physiology and Biophysics, and Pathology, University of Oklahoma Health Sciences Center and Department of Veterans Affairs Medical Center, Oklahoma City, Oklahoma; Department of Biochemistry and Molecular Biology, New Jersey Medical School, University of Medicine and Dentistry, Newark, New Jersey; and Department of Chemistry, University of Central Oklahoma, Edmond, Oklahoma, USA

Calbindin-D_{28k} gene expression in the developing mouse kidney. Calbindin-D_{28k} appears in the metanephric kidney during embryogenesis. We studied the temporal appearance and spatial distribution of calbindin-D_{28k} mRNA in the developing kidneys of 12-day fetal through 21-day postnatal mice by *in situ* hybridization. ^{35}S-UTP-labeled antisense (cRNA) probe to calbindin-D_{28k} mRNA hybridized to the ureteric buds of 12-day embryos, whereas adjacent metanephrogenic tissue was unlabeled. By embryonic day 13, Y-shaped bodies of "advancing" ureteric buds were labeled intensely. In 16-day embryos, ampullae of ureteric buds were located immediately beneath the renal capsule and labeled strongly, in contrast to metanephric tubules and S-shaped bodies. The former were unlabeled and the latter were labeled only at points of contact with the ampullae. Subsequently, the ampullae of the metanephric ureteric buds hybridized with the cRNA probe, and from the 18th embryonic to the 21st postnatal day, this labeling was intense. The cRNA probe did not hybridize with the renal vesicles, proximal tubules, or tubular segments of Henle's loop derived from nephrogenic blastema, but it did label distal nephron segments. By the 21st postnatal day, collecting ducts and ureter no longer were labeled. In conclusion, calbindin-D_{28k} mRNA is present in the developing mouse kidney, and its distribution during nephrogenesis is identical to that of calbindin-D_{28k} *per se*. Collectively, these findings show that the calbindin-D_{28k} gene is transcribed and its message is translated by the cells of the ureteric bud during the initial stage of renal morphogenesis.

Calbindin-D_{28k}, a cytosolic high-affinity calcium-binding protein, is present during embryonic development of the nephron [1–3]. In rabbits, the protein exists in the ureteric bud of the metanephric kidney on the thirteenth embryonic day [1]. During subsequent development, the ampullae of the metanephric ureteric buds contain calbindin-D_{28k}, while the protein is lost gradually from the ureters and the deep interstitial collecting ducts. Calbindin-D_{28k} is absent in the renal vesicles derived from the nephrogenic blastema, but it is present in the connecting tubules during formation of the arcades, suggesting that connecting tubules are derived from the ureteric buds [1]. A similar pattern is observed in humans [2]. Calbindin-D_{28k} is present from the eleventh week of gestation, at which time it is located in cells of all deep parts of the collecting ducts and some distal tubules in the deep cortex. S-bodies are devoid of the protein. With kidney maturation, there is a reduction in collecting duct calbindin-D_{28k} content in the deep portions of the kidney and a concomitant increase in the number of distal tubular cells that contain the protein [2]. In the mouse, calbindin-D_{28k} first appears in the metanephric duct on the twelfth day of gestation, one day after the appearance of the duct in the embryo [3]. Subsequently, calbindin-D_{9k} appears in the same distal convoluted tubule cells as calbindin-D_{28k} on the fifteenth day of embryogenesis. These proteins colocalize in distal nephron segments of the adult mouse kidney [4].

The purpose of the present study was to localize the mRNA for the calbindin-D_{28k} gene during development of the murine kidney and to compare it with the distribution of calbindin-D_{28k} *per se*.

Methods

Animals

Adult Swiss-Webster mice of both sexes were obtained from the Zoology Department at the University of Oklahoma (Norman, Oklahoma, USA), and female Swiss-Webster mice whose pregnancies had been timed were purchased from Sasco, Inc. (Omaha, Nebraska, USA). All mice were fed a standard laboratory diet (Number 8604, Teklad, Inc., Madison, Wisconsin, USA) *ad libitum*. Adult males, nonpregnant females, and neonates of zero, one, two, and three weeks of age were killed by cervical dislocation. Some adult mice were anesthetized with 60 mg of sodium pentobarbital per kg body weight and their tissues fixed by intracardiac perfusion with a paraformaldehyde (PFA) solution (*vide infra*). These animals were killed by exsanguination from the right atrium during the fixation process. Pregnant mice were killed by cervical dislocation on days 12, 13, 16, 18, and 20 following conception. The first day of appearance of a vaginal plug was counted as day 0 of gestation. Embryos were dissected from uteri under stereomicroscopic observation and fixed directly in PFA or immediately frozen in liquid nitrogen.

Radiolabeled RNA probes

^{35}S-UTP-labeled RNA probes were prepared from a 1.2-kilobase mouse cerebellar calbindin-D_{28k} sequence that was subcloned in pIBI76 [5]. The plasmid was linearized with PvuI or XbaI and antisense (cRNA) and sense RNA probes were transcribed using T7- and SP6-RNA polymerases, respectively, according to protocols provided by Promega Corp. (Madison,

Received for publication November 9, 1992
and in revised form March 2, 1993
Accepted for publication March 4, 1993

Wisconsin, USA). Following RNA probe syntheses, the templates were digested with RQ1 DNAse (1 U/μl) for 15 minutes at 37°C. The reaction products were extracted with phenol/chloroform/isoamyl alcohol (24:23:1) and purified using spun columns [6]. The RNA probes were partially hydrolyzed with 40 mM $NaHCO_3$/60 mM Na_2CO_3 for 38 minutes at 60°C to produce fragments that were approximately 200 nucleotides in length [7]. Digests were precipitated by mixing with 0.1 volume of 3 M sodium acetate and 2.5 volumes of ethanol at −20°C for two hours. This mixture was then centrifuged at 15,000 × *g* for 30 minutes and the pellet resuspended in 100 μl of diethylpyrocarbonate (DEPC)-treated water containing 20 mM dithiothreitol (DTT).

In situ *hybridization*

Whole embryos at 12, 13, and 16 days of development, or kidneys from 18- and 20-day-old embryos and neonates, were either fixed in 4% PFA in 0.1 M phosphate-buffered saline (PBS), pH 7.2, at 4°C for two hours or embedded in OCT Compound (Miles Inc., West Haven, Connecticut, USA) and frozen in liquid nitrogen. Some PFA-fixed tissues were immersed in 15% sucrose in 0.1 M PBS overnight at 4°C and subsequently embedded in OCT Compound and frozen in liquid nitrogen. Other PFA-fixed specimens were washed in PBS for 15 minutes, dehydrated in aqueous solutions with increasing ethanol concentrations, immersed in xylene, and embedded in paraffin wax. Nonpregnant female and male adult mice were anesthetized and perfused through the heart with 4% PFA in PBS at 4°C for 20 minutes. The kidneys were removed, sliced into 3 mm-thick sections, and fixed for an additional two hours by immersion in 4% PFA in 0.1 M PBS at 4°C. Slices were then processed either for frozen or paraffin sectioning as described above. Paraffin- and OCT-embedded tissue blocks were stored at −20 and −70°C, respectively, prior to microtomy. Eight μm-thick frozen sections were prepared using a cryomicrotome (Hacker Instruments, Inc., Fairfield, New Jersey, USA). Five μm-thick paraffin sections were cut with a Reichert-Jung 2040 microtome (Cambridge Instruments, Inc., Deerfield, Illinois, USA). Sections were mounted on glass microscope slides that had been cleaned with 8% nitric acid, washed thoroughly with deionized water, treated in 0.1% aqueous DEPC overnight, dried at 100°C for 15 minutes, and dipped in 0.005% aqueous poly-L-lysine (frozen sections) or 2% 3-aminopropyltriethoxylsilane in acetone (paraffin sections). Sections were stored at −70°C prior to pre-treatment washes as follows. Paraffin sections were immersed in xylene and rehydrated in ethanol solutions containing increasing concentrations of water. Frozen cryostat sections were brought to room temperature under a stream of cool air. Unfixed frozen sections were immersed in 3% PFA in 0.1 M PBS for five minutes and then washed for two minutes in 0.1 M PBS. Subsequently, all sections were washed in 0.3 M NaCl and 0.03 M Na citrate (2× SSC) for two minutes and acetylated for 20 minutes in 0.1 M triethanolamine (pH 8.0) containing 0.1% acetic anhydride. Sections were then briefly rinsed in 2× SSC and 0.1 M PBS and then immersed in a solution of 0.1 M glycine and 0.1 M Tris · HCl (pH 7.0) for 30 minutes. They were rinsed briefly in 2× SSC, dehydrated in solutions of increasing ethanol concentrations, and air dried. Slides were stored at −70°C until hybridization. Fifty μl of hybridization mixture (40% deionized formamide, 10% dextran sulfate, 10 mM DTT, 1 mg/ml yeast tRNA, 1 mg/ml sheared salmon sperm DNA, 1× Denhardt's solution, and 4× SSC), containing 2.5 × 10^5 dpm of either ^{35}S-UTP-labeled sense or antisense RNA, were applied per slide and covered with Parafilm. Slides were placed in a humidified chamber at 50°C for 3.5 hours. Following hybridization, the Parafilm was removed and the sections were briefly washed twice with 2× SSC. After immersion in 50% deionized formamide/2× SSC at 50°C, first for five and then for 20 minutes, the sections were briefly rinsed in 2× SSC and then treated with 100 μg/ml RNAse A in 2× SSC for 30 minutes at 37°C. The sections were then placed in 50% deionized formamide at 52°C for five minutes and then in 2× SSC/0.05% Triton X-100 overnight on a rocker table. The sections were subsequently dehydrated with solutions of increasing ethanol concentrations containing 300 mM ammonium acetate and air dried. Radioautography was performed with NTB2 emulsion (Eastman Kodak Co., Rochester, New York, USA) according to the manufacturer's instructions. Slides were placed in light-tight slide boxes at 4°C for two to three weeks and then were developed and counterstained with hemotoxylin and eosin. Sections were mounted with Permount (Fisher Scientific, Fair Lawn, New Jersey, USA), covered with glass coverslips, and examined by both bright- and dark-field microscopy using a Model BH-2 Olympus microscope (Olympus Corp., Lake Success, New York, USA). Photomicrographs were taken with an Olympus Model PM-10-ADS camera system using TMAX Black-and-White Print Film or Kodak Ektar 100 Color Print Film.

Quantitative radioautography

Dark-field photomicrographs of tissue sections were enlarged to 8 inch × 10 inch black-and-white prints. Areas were outlined on a SummaSketch II Professional digitizing pad (SummaGraphics Corp., Fairfield, Connecticut, USA) and were quantitated with a Ceptre 386 personal computer using IBM PC-compatible software for three-dimensional reconstruction of planar images (distributed by the University of Denver, Denver, Colorado, USA) [8]. Measurements were made only in a single plane. The numbers of silver grains overlying demarcated areas were counted visually. The number of background grains, measured over glass away from tissue sections, are presented separately and are not subtracted from the values appearing in Tables 1 through 3. Grain densities expressed per cell were determined by counting grains over specific structures and dividing these results by the number of nuclei. Results are presented as the mean ± SE. Statistical inferences were derived from one-way analysis of variance [9] in conjunction with the Bonferroni *t*-test for comparison of multiple means [10] or the *t* statistic for two means [11]. *P* values less than 0.05 were considered significant and are indicated in the tables by an asterisk.

Chemicals

Chemicals were obtained from the following sources: radionucleotides (New England Nuclear Research Products, Boston, Massachusetts, USA); RNA polymerases, restriction enzymes, and RQ1 DNAse (Promega, Madison, Wisconsin, USA); agarose (Bio-Rad, Richmond, Virginia, USA); DEPC, dextran

Table 1. Silver grain densities over adult mouse kidney hybridized with ^{35}S-UTP-labeled cRNA for calbindin-D_{28k}

Structure	Grains/μm^2			Grains/cell		
	Antisense		Sense	Antisense		Sense
Fresh frozen						
Distal tubule	0.255 ± 0.019^a ($N = 22$)	*	0.066 ± 0.002^c ($N = 6$)	28.7 ± 1.7^b ($N = 22$)	*	1.3 ± 0.2^d ($N = 6$)
Proximal tubule	0.017 ± 0.002^a ($N = 18$)	*	0.067 ± 0.004^c ($N = 6$)	1.9 ± 0.2^b ($N = 18$)	*	2.2 ± 0.1^d ($N = 6$)
Glomerulus	0.017 ± 0.001^a ($N = 12$)	*	0.074 ± 0.004^c ($N = 6$)	1.2 ± 0.1^b ($N = 12$)	*	0.9 ± 0.04^d ($N = 6$)
Vascularly perfused						
Distal tubule	0.437 ± 0.016^e ($N = 15$)	*	0.027 ± 0.002^g ($N = 6$)	23.4 ± 0.7^f ($N = 15$)	*	2.2 ± 0.4^h ($N = 6$)
Proximal tubule	0.042 ± 0.006^e ($N = 15$)	*	0.025 ± 0.002^g ($N = 6$)	2.8 ± 0.2^f ($N = 15$)	*	2.3 ± 0.2^h ($N = 6$)
Glomerulus	0.013 ± 0.002^e ($N = 7$)	*	0.025 ± 0.003^g ($N = 6$)	0.8 ± 0.04^f ($N = 7$)	*	2.0 ± 0.1^h ($N = 6$)

Background values in emulsion over glass for antisense and sense RNA probes were 0.0067 ± 0.0008 and 0.0085 ± 0.0008 grains/μm^2, respectively, for fresh frozen tissue and 0.0075 ± 0.0003 and 0.0116 ± 0.0008 grains/μm^2, respectively, for tissues fixed by vascular perfusion. F values for analysis of variance of groups a through h were 103.7*, 161.5*, 1.27, 32.4*, 427.9*, 566.4*, 0.4, and 0.3, respectively. * $P < 0.05$ for F values and for comparisons between values bracketing asterisks.

Table 2. Silver grain densities over embryonic mouse kidney hybridized with ^{35}S-UTP-labeled cRNA for calbindin-D_{28k}

Structure	Grains/μm^2		
	13th gestational day		16th gestational day
Ureteric bud	0.250 ± 0.007^a ($N = 8$)	*	0.145 ± 0.007^b ($N = 9$)
Metanephric blastema	0.035 ± 0.002^a ($N = 8$)	*	0.023 ± 0.001^b ($N = 9$)
Metanephric tubule	$0.028 \pm 0.002^{a,c}$ ($N = 8$)	*	$0.021 \pm 0.002^{b,c}$ ($N = 9$)
S-shaped body			$0.021 \pm 0.002^{b,d}$ ($N = 6$)

All tissues were fresh frozen. Sense RNA values for ureteric bud, metanephric blastema, and collecting duct were 0.016 ± 0.001, 0.013 ± 0.001, and 0.015 ± 0.001, respectively, on the 13th day of gestation ($F = 2.1$).

F values for groups a and b were 736.4* and 216.2*, respectively. * $P < 0.05$ for values bracketing asterisks and for c (ureteric bud versus metanephric tubule) and d (ureteric bud versus S-shaped body).

Table 3. Silver grain densities over neonatal mouse kidney hybridized with ^{35}S-UTP-labeled cRNA for calbindin-D_{28k}

Structure	Grains/μm^2		
	Antisense		Sense
1-day-old mice			
Distal tubule	0.123 ± 0.013^a	*	0.017 ± 0.002^b
Proximal tubule	0.030 ± 0.003^a		0.023 ± 0.003^b
Glomerulus	0.028 ± 0.002^a	*	0.017 ± 0.003^b
1-week-old mice			
Distal tubule	0.149 ± 0.015^c	*	0.022 ± 0.003^d
Proximal tubule	0.031 ± 0.004^c	*	0.051 ± 0.006^d
Glomerulus	0.031 ± 0.002^c	*	0.056 ± 0.003^d
2-week-old mice			
Distal tubule	0.248 ± 0.015^e	*	0.049 ± 0.006^f
Proximal tubule	0.028 ± 0.002^e	*	0.052 ± 0.004^f
Glomerulus	0.028 ± 0.001^e	*	0.031 ± 0.001^f
3-week-old mice			
Distal tubule	0.315 ± 0.022^g	*	0.025 ± 0.002^h
Proximal tubule	0.024 ± 0.004^g		0.026 ± 0.001^h
Glomerulus	0.027 ± 0.004^g		0.028 ± 0.002^h

Background values in emulsion over glass for antisense and sense RNA probes were 0.001 and nil, 0.006 ± 0.001 and 0.013 ± 0.001, and 0.017 ± 0.001 and 0.019 ± 0.001 grains/μm^2, respectively, for one-day-old, one-week-old, and two-week-old mice. All tissues were fresh frozen, and $N = 6$ for each group.

F values for analysis of variance of groups a through h were 51.8*, 1.6, 55.8*, 18.7*, 201.7*, 7.0*, 185.1*, and 0.3, respectively. * $P < 0.05$ for F values and for comparisons between values bracketing asterisks.

sulfate, DTT, ethidium bromide, acetic anhydride, poly-L-lysine, 3-aminopropyltriethoxylsilane, Tris HCl, glycine, mono- and dibasic sodium phosphates, yeast tRNA, sheared salmon sperm DNA, and RNAse (Sigma, St. Louis, Missouri, USA); triethanolamine, NTB2 emulsion, and TMAX and Ektar 100 films (Eastman Kodak Co., Rochester, New York, USA); sodium acetate, formamide, and PFA (Mallinckrodt, Paris, Kentucky, USA); and sodium pentobarbital (Vetlabs, Lenexa, Kansas, USA).

Results

In adult mouse kidneys fixed by immersion in either liquid nitrogen or PFA, concentrations of silver grains—indicating binding of the cRNA probe to calbindin-D_{28k} mRNA—were located over discrete tubular cells within the cortex (Fig. 1A). In contrast, sections incubated with sense (control) RNA demonstrated a homogeneous distribution of silver grains whose low density was similar to that observed over unlabeled structures in sections hybridized with the cRNA probe (Fig. 1B). In kidneys fixed by vascular perfusion with PFA, silver grains were concentrated over cells of the distal convoluted and connecting tubules, while proximal tubules were labeled only with background levels of silver grains (Fig. 2). Table 1 summarizes the silver grain densities over structures in the renal

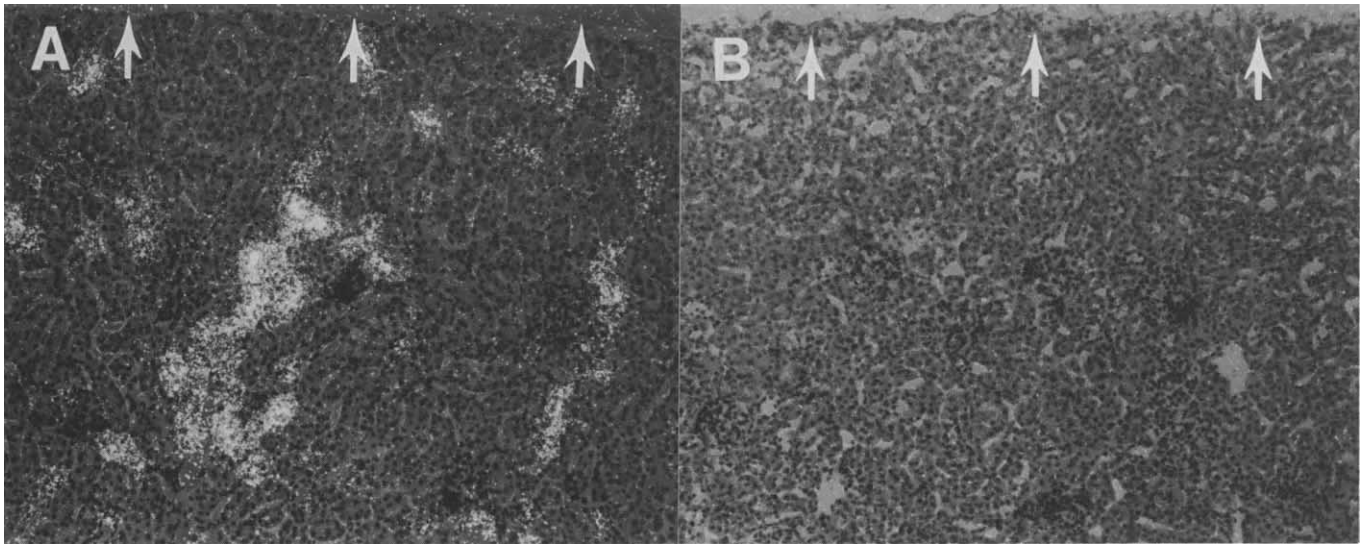

Fig. 1. *Dark-field photomicrographs of fresh-frozen adult mouse kidney cortex hybridized with ^{35}S-UTP-labeled antisense RNA (A) or sense (control) RNA (B) for calbindin-D_{28k}.* Capsule is indicated by arrows. Each section was exposed for 3 weeks. Magnification = 106×

cortex of adult mice. In both fresh-frozen and vascularly perfused tissue, cRNA to calbindin-D_{28k} mRNA localized primarily in distal tubules.

At the twelfth gestational day the nephrogenic cord was radiolabeled along its entirety. Cells of the metanephrogenic cord, which were not yet organized into renal vesicles, were unlabeled. In contrast, signal for calbindin-D_{28k} mRNA was prominent over the ureteric bud in each developing kidney. Mesonephric tubules also were labeled. By the thirteenth embryonic day, the kidney was delimited by its capsule, and Y-shaped bodies of individual ureteric buds, including ampullae with lumina, were labeled intensely (Figs. 3 and 4). Neither the developing metanephric tubules nor the metanephric blastema showed detectable mRNA for calbindin-D_{28k}. On the sixteenth embryonic day, the ampullae, which continued to be labeled intensely, were located immediately beneath the metanephric renal capsule (Fig. 5). Neither glomeruli nor unidentified metanephric tubules were labeled. S-shaped vesicles began to appear on the sixteenth embryonic day. Labeling was observed over the cells of the ampullae of the ureteric buds as well as over the inner metanephric cord cells abutting the ampullae (Fig. 5). The majority of the cells within S-shaped vesicles were unlabeled (Fig. 5). A similar pattern of positively labeled ureteric buds with minimally labeled metanephric tissue elements was observed in all embryonic kidneys. Table 2 summarizes the silver grain densities over structures of the embryonic kidney at the thirteenth and sixteenth days of gestation. All ureteric buds included for analysis in this table were located immediately beneath the metanephric kidney capsule. By the eighteenth day of gestation, the ampullae were labeled exclusively and were situated immediately beneath the renal capsule (Fig. 6). After 21 days of gestation, which is the birth date for these mice, individual distal tubules were present, and their cells contained mRNA for calbindin-D_{28k}. In the kidneys of one- and two-week old animals, the cortex was beginning to segregate from the medulla and labeled structures were observed only in the cortex (Fig. 7). Higher magnification revealed selective labeling of cells solely within the distal nephron (Fig. 8). At three weeks of age, labeling for calbindin-D_{28k} mRNA was present in distal convoluted and connecting tubules in the outer cortex (Fig. 9A, B), but was absent from the collecting ducts (Fig. 9C, D). Table 3 summarizes silver grain densities over structures of neonatal mouse kidneys.

The distribution of calbindin-D_{28k} mRNA in embryos prior to 12 days of gestation was examined in fresh-frozen tissue sections, but the indistinct structure of these specimens precluded interpretation of these observations.

Discussion

In the present study calbindin-D_{28k} mRNA was detected in the murine kidney from the twelfth day of gestation through adulthood. During embryonic and early postnatal development, it localized selectively to the "advancing" ampullae of the ureteric buds, and in adulthood, it was found in the distal nephron. The temporal appearance and structural localization of calbindin-D_{28k} mRNA correspond closely to those of calbindin-D_{28k} *per se* in developing rabbit and mouse kidneys [1, 3]. Collectively, these studies show that the gene for calbindin-D_{28k} is transcribed and its message translated by cells of the advancing ampullae of the ureteric bud during the initial stages of renal morphogenesis.

A question raised by the present study is: at what point in time do distal convoluted tubules, which are derived from the metanephric blastema, form and express mRNA for calbindin-D_{28k}? Current evidence suggests that connecting tubules are derived from the ureteric bud, whereas all preceding nephron segments, including distal convoluted tubules *per se*, are derived from the renal vesicle [1]. The latter, in turn, originates from the metanephric blastema [1]. In the present study metanephric blastema generally was unlabeled. However, careful inspection of Figure 5 shows that silver grains are present over

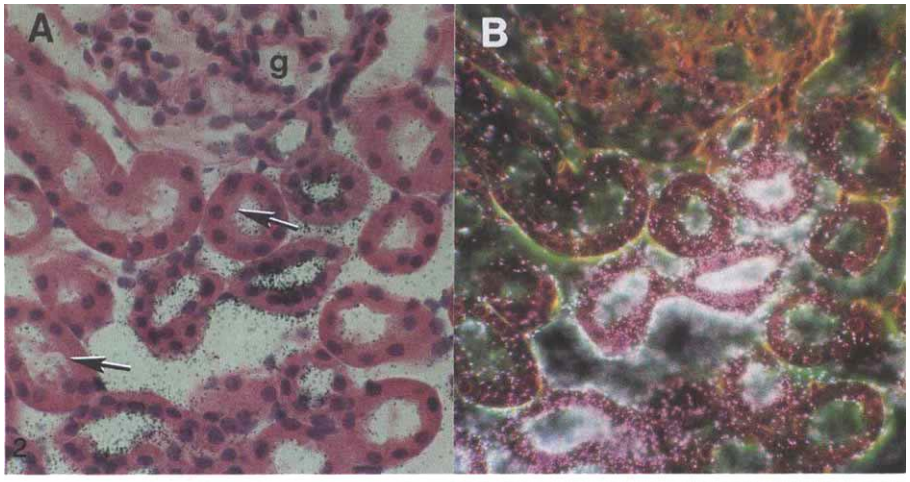

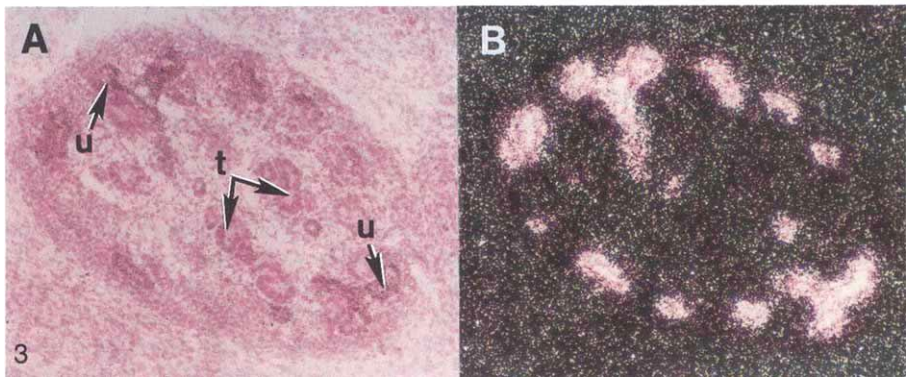

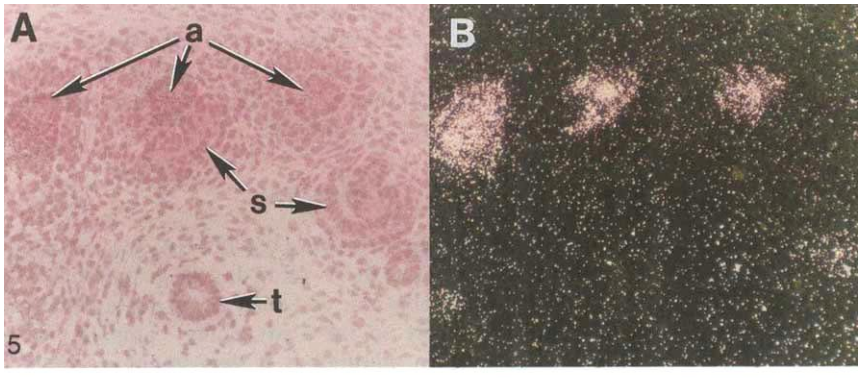

Fig. 2. *Bright- (A) and dark- (B) field photomicrographs of perfusion-fixed, paraffin-embedded, adult mouse kidney hybridized with calbindin-D_{28k} cRNA.* Proximal tubules are characterized by a brush border (arrows) and basally-located nuclei which are fewer in number than in distal tubular cells (A). Silver grains over distal tubules are most easily seen with dark-field illumination (B). Abbreviation is g, glomerulus. Magnification = 525×

Fig. 3. *Bright- (A) and dark- (B) field photomicrographs of fresh-frozen fetal kidney at 13th day of gestation hybridized with calbindin-D_{28k} cRNA.* Grains are restricted to developing ureteric buds (u). Metanephric tubules (t) and metanephrogenic blastema exhibit only background signal. Magnification = 125×

Fig. 5. *Bright- (A) and dark- (B) field photomicrographs of fresh-frozen fetal kidney at 16th day of gestation hybridized with calbindin-D_{28k} cRNA.* Silver grains are present over the cells of the "advancing" ampullae (a) of the ureteric buds and the margins of the condensing metanephrogenic blastema but are absent from S-shaped bodies (s) and the metanephric tubules (t). Outermost margin of the metanephros is at the level of the letter "A" in the bright-field photomicrograph. Magnification = 209×

Fig. 6. *Dark-field photomicrograph of PFA-fixed, paraffin-embedded, fetal kidney at 18th day of gestation hybridized with calbindin-D_{28k} cRNA.* The ampullae located at the outer margin are labeled by silver grains (pink). Developing glomeruli and metanephric tubules are unlabeled. Abbreviation is ad, adrenal gland. Magnification = 104×

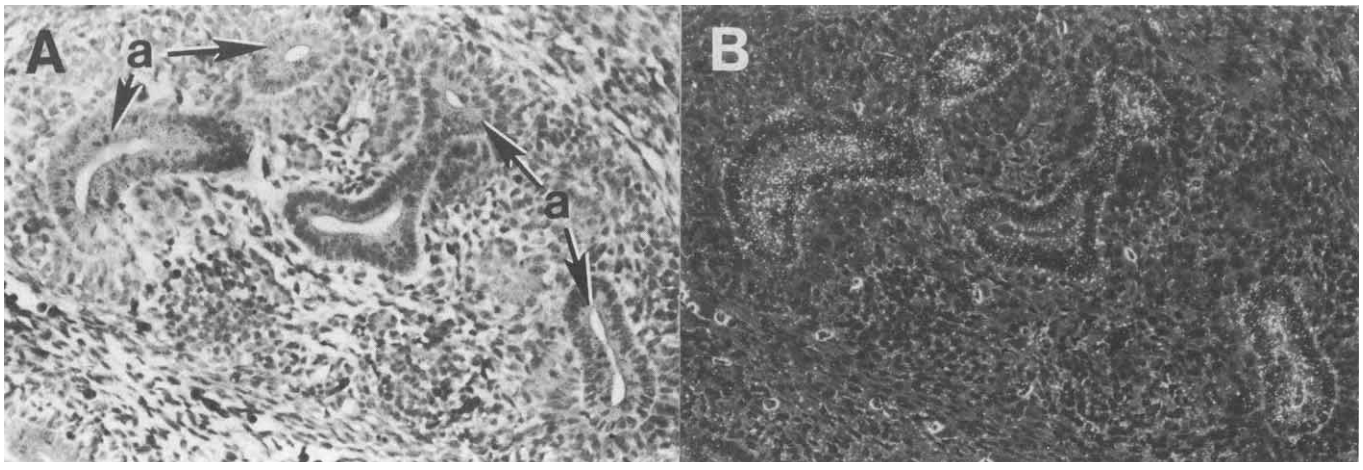

Fig. 4. *Bright- (A) and dark- (B) field photomicrographs of PFA-fixed, paraffin-embedded, fetal kidney at 13th day of gestation hybridized with calbindin-D_{28k} cRNA.* Silver grains are restricted to ampullae (a) of ureteric buds. The surrounding metanephrogenic blastema does not show specific hybridization. Magnification = 87×

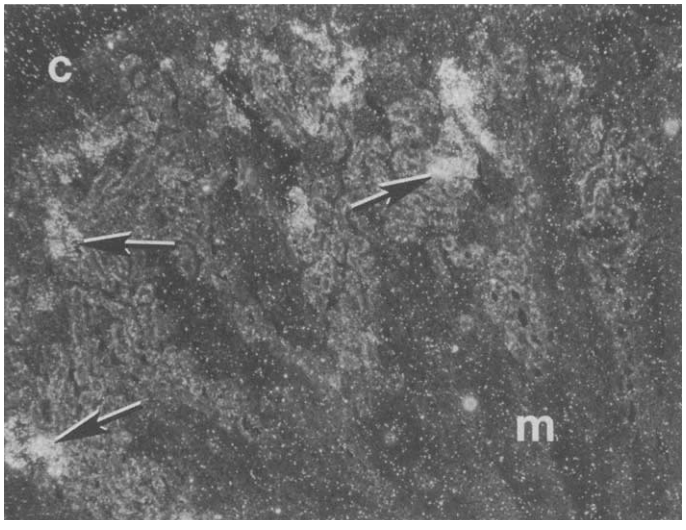

Fig. 7. *Dark-field photomicrograph of fresh-frozen, one-week-old, neonatal kidney hybridized with calbindin-D_{28k} cRNA.* Silver grains are concentrated over distal tubules (arrows). Abbreviations are: c, capsule; m, medulla. Magnification = 80×

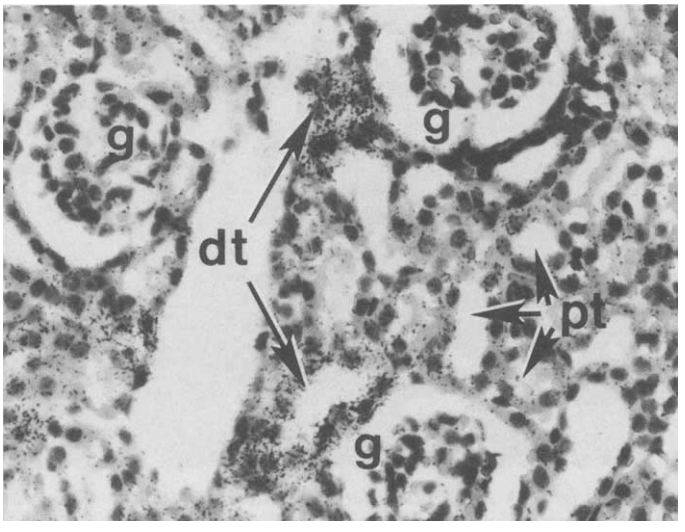

Fig. 8. *Bright-field photomicrograph of PFA immersion-fixed, paraffin-embedded, two-week-old, neonatal mouse kidney hybridized with calbindin-D_{28k} cRNA.* Silver grains are most dense over distal tubules (dt). Background silver grains are present over proximal tubules (pt) and glomeruli (g). Magnification = 203×

the margins of condensing metanephric blastema around labeled "advancing" ampullae, suggesting activation of the calbindin-D_{28k} gene in cells that may be destined to comprise the distal convoluted tubule. This hypothesis is speculative at present and requires further experimental investigation.

Silver grain densities were quantitated in the present study, allowing comparison with a previous investigation of gene expression in the adult murine kidney [12]. Although differences in technique (such as, cRNA probe concentration and radioactivity, exposure time, and differences in fixation) preclude absolute comparisons, qualitatively the results were similar. In the adult mouse kidney, mRNA for calbindin-D_{28k} localized primarily over distal tubular segments and was essentially absent from both glomeruli and proximal tubules (compare Tables 1 and 2 of [12] to Table 1 of the present study). In embryonic mouse kidney, calbindin-D_{28k} mRNA localized primarily over the ureteric bud on both the thirteenth and sixteenth days of gestation. Following birth, grain densities over distal tubules increased with time (Table 3), consistent with quantitative slot blot hybridization analyses of whole kidneys from neonatal mice demonstrating an increase in calbindin-D_{28k} mRNA levels between birth and three weeks of age [13]. We presently have no explanation for why modestly higher silver grain densities were observed with radiolabeled sense than anti-sense RNA in proximal tubules and glomeruli of adult mouse fresh-frozen kidney sections (Table 1) or in one-week-old neonatal mice (Table 3).

The present study confirms that calbindin-D_{28k} mRNA is

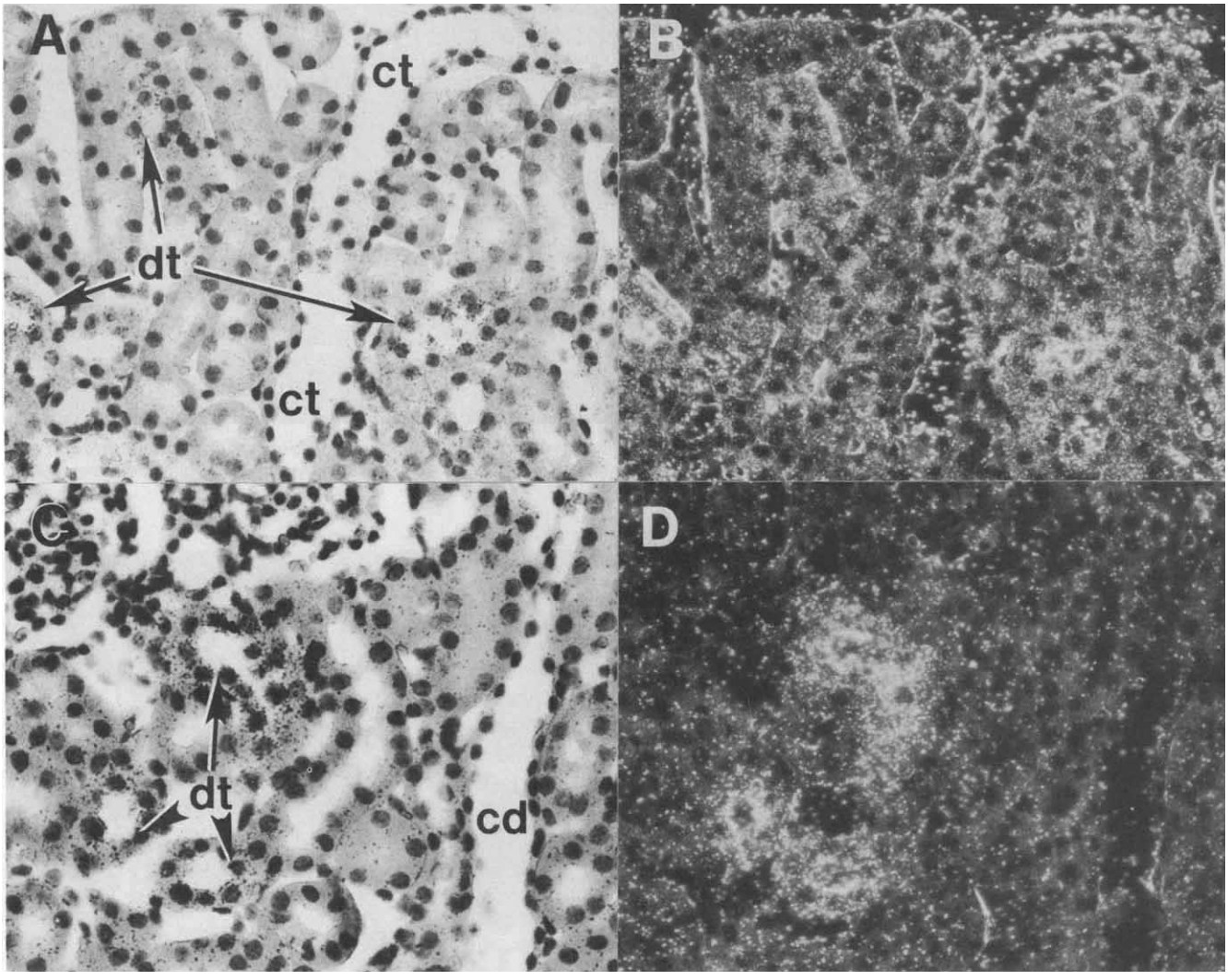

Fig. 9. *Bright- (A and C) and dark- (B and D) field photomicrographs of PFA immersion-fixed, paraffin-embedded, three-week-old, neonatal kidney, hybridized with calbindin-D_{28k} cRNA.* Silver grains in B and D are concentrated over distal nephron segments (dt), including both distal convoluted (arrows) and connecting tubules (ct). In contrast, collecting ducts (cd) demonstrate grain densities similar to background. Magnification = 203×

present only in cells of the distal nephron in the adult mouse kidney [12]. Although the previous study differentiated between proximal and distal portions of the mouse nephron, it was not possible to identify discrete segments of the distal tubule, such as, the distal convoluted tubule, the connecting tubule, and the early cortical collecting duct [14]. Improved preservation of structural detail with vascular perfusion fixation in the present study showed that mRNA for calbindin-D_{28k} is expressed in the cells of the distal convoluted and connecting tubules and is absent from cells of the cortical collecting ducts, consistent with the localization of calbindin-D_{28k} itself in these structures [15].

A summary of studies localizing calbindin-D_{28k} by immunocytochemistry and calbindin-D_{28k} mRNA by *in situ* hybridization in developing and mature kidneys of different mammalian species is presented in Table 4. Collectively, they demonstrate coordinate expression, both temporally and spatially, of the mRNA and the protein encoded by the calbindin-D_{28k} gene in the kidney during embryogenesis and adulthood.

In conclusion, the gene for calbindin-D_{28k} is expressed during ontogeny of the murine nephron. It is both transcribed and translated in cells of the "advancing" ampullae of ureteric buds from the first stages of metanephric development through the third week following birth. The regulation of this gene and its role, if any, in nephrogenesis remain to be elucidated.

Acknowledgments

This work was supported in part by National Institutes of Health grants DK35985 (JEB) and DK38961 (SC) and the Molecular Pathology Core Laboratory of the Oklahoma Center for Molecular Medicine, University of Oklahoma Health Sciences Center, Oklahoma City, Oklahoma. We thank Professor Brigitte Kaissling for help with the microanatomy of the adult mouse kidney. The technical assistance of Geraldine A. Chissoe and the staffs of the Molecular Pathology Core Laboratory and the Samuel Roberts Noble Microscopy Laboratory,

Table 4. Summary of studies localizing calbindin-D_{28k} and its messenger RNA in mammalian kidneys

Authors	Reference	Species/gender/age/location
Calbindin-D_{28k}		
Chandler and Bucci	16	rat/♀, ♂/E10-P7/distal tubules (beginning day E19)
Rhoten and Christakos	17	rat/♂/P12/thick ascending limbs of Henle's loop and distal tubules rat/♂/7-weeks/distal convoluted tubules
Taylor et al	18	rat/♀/adult/distal convoluted tubules, connecting tubules, cortical collecting ducts (rare) rabbit/♀, ♂/adult/distal convoluted tubules, connecting tubules, cortical collecting ducts (rare)
Roth et al	19	rat/♂/~1 year/distal convoluted tubules, connecting tubules, initial cortical collecting ducts, medullary collecting ducts (rare) human/♀, ♂/2.5 to 50 years/same as rat plus 50% of cells in medullary collecting ducts
Schreiner et al	20	rat/♂/4-weeks/distal convoluted tubules, connecting tubules, initial cortical collecting ducts pig and human/unknown/adult and unknown/same as rat monkey/unknown/unknown/same as rat plus entire length of collecting ducts
Rhoten et al	4	rat/unknown/P-12 and ≥7-weeks/distal convoluted tubules, connecting tubules mouse/unknown/unknown/distal convoluted tubules, connecting tubules, cortical collecting ducts
McIntosh et al	1	rabbit/♀, ♂/E13-P17/ampullae of metanephric ureteral buds
Mounier et al	2	human/unknown/E77 to 32 years/deep collecting ducts during early fetal development; distal convoluted tubules, connecting tubules, and collecting ducts in adults
Séquier et al	21	rat/♂/adult/distal tubules
Borke et al	22	human/unknown/unknown/distal convoluted tubules, connecting tubules, cortical collecting ducts
Borke et al	23	rat/unknown/adult/distal convoluted tubules, connecting tubules, portions of cortical collecting ducts
Christakos et al	15	mouse/unknown/adult/distal convoluted tubules, connecting tubules, cortical collecting ducts
Opperman et al	24	baboon/unknown/adult/distal convoluted tubules, connecting tubules, medullary and cortical collecting ducts
Bindels et al	25	rat/♂/adult/distal convoluted tubules, connecting tubules
Bindels et al	26	rat/♂/adult/distal convoluted tubules, connecting tubules
Shamley et al	3	mouse/E11-P2/unknown/metanephric duct cells (beginning E12), distal tubule cells (beginning E15)
Calbindin-D_{28k} messenger RNA		
Séquier et al	21	rat/♂/adult/distal tubules
Rhoten and Christakos	12	mouse/♂/≥4-weeks/distal tubules
Present study		mouse/♀, ♂/E12-P21/ampullae of metanephric ureteric buds in fetal kidneys, distal convoluted tubules and connecting tubules postnatally

Abbreviations are: ♀, female; ♂, male; E, embryonic day; P, postnatal day.

University of Oklahoma, Norman, Oklahoma are gratefully acknowledged. Portions of this study were presented at the 25th annual meeting of the American Society of Nephrology.

Reprint requests to Dr. James E. Bourdeau, Section of Nephrology (111G), Room 2E-106, Department of Veterans Affairs Medical Center, 921 Northeast Street, Oklahoma City, Oklahoma 73104-5028, USA.

References

1. McIntosh JE, Bourdeau JE, Taylor AN: Immunohistochemical localization of calbindin-D_{28k} during development of the rabbit nephron. *Anat Rec* 215:383–389, 1986
2. Mounier F, Hinglais N, Bréhier A, Thomasset M, Lacoste M, Sich M, Gubler M-C: Ontogenesis of 28 kDa vitamin D-induced calcium-binding protein in human kidney. *Kidney Int* 31:121–129, 1987
3. Shamley DR, Opperman LA, Buffenstein R, Ross FP: Ontogeny of calbindin-D_{28k} and calbindin-D_{9k} in the mouse kidney, duodenum, cerebellum and placenta. *Development* 116:491–496, 1992
4. Rhoten WB, Bruns ME, Christakos S: Presence and localization of two vitamin D-dependent calcium-binding proteins in kidneys of higher vertebrates. *Endocrinol* 117:674–683, 1985
5. Wood TL, Kobayashi Y, Frantz G, Varghese S, Christakos S, Tobin AJ: Molecular cloning of the mammalian 28,000 M_r vitamin D-dependent calcium binding protein (calbindin-D_{28k}): Expression of calbindin-D_{28k} RNAs in rodent brain and kidney. *DNA* 7:585–593, 1988
6. Sambrook J, Fritsch EF, Maniatis T: *Molecular Cloning: A Laboratory Guide* (2nd ed). Cold Spring Harbor, Cold Spring Harbor Laboratory Press, 1989, p. E.37
7. Cox KH, DeLeon DV, Angerer LM, Angerer RC: Detection of mRNAs in sea urchin embryos by *in situ* hybridization using asymmetric RNA probes. *Developmental Biol* 101:485–502, 1984
8. Young SJ, Royer SM, Groves PM, Kinnamon JC: Three dimension reconstructions from serial micrographs using the IBM-PC. *J Microsc Tech* 6:207–218, 1987
9. Freund JE: *Mathematical Statistics*. Englewood Cliffs, Prentice Hall, 1962
10. Glantz SA: *Primer of Biostatistics*. New York, McGraw Hill, 1981

11. BROWNLEE KA: *Statistical Theory and Methodology in Science and Engineering*. New York, John Wiley & Sons, 1965
12. RHOTEN WB, CHRISTAKOS S: Cellular gene expression for calbindin-D_{28k} in mouse kidney. *Anat Rec* 227:145–151, 1990
13. LI H, CHRISTAKOS S: Differential regulation by 1,25-dihydroxyvitamin D_3 of calbindin-D_{9k} and calbindin-D_{28k} gene expression in mouse kidney. *Endocrinol* 128:2844–2852, 1991
14. GUDER WG, HALLBACH J, FINK E, KAISSLING B, WIRTHENSOHN G: Kallikrein (kininogenase) in the mouse nephron: Effect of dietary potassium. *Biol Chem Hoppe-Seyler* 368:637–645, 1987
15. CHRISTAKOS S, GABRIELIDES C, RHOTEN WB: Vitamin D-dependent calcium binding proteins: chemistry, distribution, functional considerations, and molecular biology. *Endocrine Rev* 10:3–26, 1989
16. CHANDLER JS, BUCCI TJ: The ontogenesis of calcium-binding protein in fetal rat kidney. *Cell Tiss Res* 191:363–365, 1978
17. RHOTEN WB, CHRISTAKOS S: Immunocytochemical localization of vitamin D-dependent calcium binding protein in mammalian nephron. *Endocrinol* 109:981–983, 1981
18. TAYLOR AN, MCINTOSH JE, BOURDEAU JE: Immunocytochemical localization of vitamin D-dependent calcium-binding protein in renal tubules of rabbit, rat, and chick. *Kidney Int* 21:765–773, 1982
19. ROTH J, BROWN D, NORMAN AW, ORCI L: Localization of the vitamin D-dependent calcium-binding protein in mammalian kidney. *Am J Physiol* 243:F243–F252, 1982
20. SCHREINER DS, JANDE SS, PARKES CO, LAWSON DEM, THOMASSET M: Immunocytochemical demonstration of two vitamin D-dependent calcium-binding proteins in mammalian kidney. *Acta Anat* 117:1–14, 1983
21. SÉQUIER J-M, HUNZIKER W, RICHARDS G: Localization of calbindin D28 mRNA in rat tissues by *in situ* hybridization. *Neurosci Lett* 86:155–160, 1988
22. BORKE JL, MINAMI J, VERMA AK, PENNISTON JT, KUMAR R: Co-localization of erythrocyte Ca^{++}-Mg^{++} ATPase and vitamin D-dependent 28-kDa-calcium binding protein. *Kidney Int* 34:262–267, 1988
23. BORKE JL, CARIDE A, VERMA AK, PENNISTON JT, KUMAR R: Plasma membrane calcium pump and 28-kDa calcium binding protein in cells of rat kidney distal tubules. *Am J Physiol* 257:F842–F849, 1989
24. OPPERMAN LA, PETTIFOR JM, ROSS FP: Immunohistochemical localization of calbindins (28K and 9K) in the tissues of the baboon *Papio ursinus*. *Anat Rec* 228:425–430, 1990
25. BINDELS RJM, TIMMERMANS JAH, HARTOG A, COERS W, VAN OS CH: Calbindin-D_{9k} and parvalbumin are exclusively located along basolateral membranes in rat distal nephron. *J Am Soc Nephrol* 2:1122–1129, 1991
26. BINDELS RJM, HARTOG A, TIMMERMANS JAH, VAN OS CH: Immunocytochemical localization of calbindin-D_{28k}, calbindin-D_{9k} and parvalbumin in rat kidney. *Contrib Nephrol* 91:7–13, 1991